Comments on Inorganic Chemistry
Publication details, including instructions for authors and subscription information:
http://www.informaworld.com/smpp/title~content=t713455155

Rate-Constant Expressions for Nonadiabatic Electron-Transfer Reactions

Bruce S. Brunschwig[a]; Norman Sutin[a]
[a] Department of Chemistry, Brookhaven National Laboratory, Upton, New York

To cite this Article Brunschwig, Bruce S. and Sutin, Norman(1987) 'Rate-Constant Expressions for Nonadiabatic Electron-Transfer Reactions', Comments on Inorganic Chemistry, 6: 4, 209 — 235
To link to this Article: DOI: 10.1080/02603598708072291
URL: http://dx.doi.org/10.1080/02603598708072291

Rate-Constant Expressions for Nonadiabatic Electron-Transfer Reactions

Expressions for the rate constants for nonadiabatic electron-transfer reactions are presented. These expressions are valid when the electronic coupling between the two redox sites is small and the energy surfaces for the initial and final states are harmonic with identical force constants. High- and low-temperature limiting forms of the rate equations are presented and closed-form expressions which are good approximations to the Franck–Condon sums appearing in these equations are described. Systems in which the electron transfer causes a displacement in one or more vibrational modes are considered. When several vibrational modes are "active," the higher frequency modes have different effects on the rate constants in the normal and inverted free-energy regions. In the inverted region nuclear tunneling effects are large when $\hbar\omega_f > 2kT$. Under these conditions the rate has only a weak dependence on temperature and the rate constants can exhibit "quantum beats." Nuclear tunneling effects are smaller in the normal region: the rate has a stronger dependence on temperature and quantum beats are not observed.

There is currently considerable interest in the distance and temperature dependence of electron-transfer rates.[1–3] Electon transfer occurs over relatively large distances in photosynthesis and in a variety of biological, chemical and physical processes.[4–8] In such systems the electronic coupling of the two redox sites is very weak and the electron transfer is nonadiabatic. At high temperatures such reactions can be treated in terms of an activated-complex framework but at low temperatures nuclear tunneling contributions to the rate can be very important. Although corrections for nuclear tunneling can be introduced into the activated-complex treatment,

Comments Inorg. Chem.
1987, Vol. 6, No. 4, pp. 209–235
Photocopying permitted by license only

nuclear tunneling enters naturally in a quantum-mechanical description, and such a treatment will be used here.

Nonadiabatic electron transfers in which there is appreciable nuclear tunneling are conveniently considered in terms of the formalism developed for multiphonon radiationless transitions.[1,2,9–14] In this formalism the probability per unit time that a system in an initial vibronic state Av will undergo a transition to a set of vibronic levels $\{Bw\}$ is given by

$$W_{Av} = \frac{2\pi H_{AB}^2}{\hbar} \sum_w S_{Av,Bw}^2 \delta(\epsilon_{Av} - \epsilon_{Bw}) \tag{1}$$

where H_{AB} is the electronic coupling matrix element, $S_{Av,Bw}$ is the square of the overlap of the vibrational wavefunctions, ϵ_{Av} and ϵ_{Bw} are the energies of the vibrational levels, and the delta function ensures energy conservation. It is assumed that only two electronic states, one for the reactants and one for the products, need to be considered. If a Boltzmann distribution over the vibrational energy levels (including those of the solvent oscillators) of the initial electronic state A is assumed, the thermally averaged probability per unit time of passing from a set of vibrational levels $\{Av\}$ of the initial electronic state to a set of vibrational levels $\{Bw\}$ of the final electronic state B is

$$k = \frac{2\pi H_{AB}^2}{\hbar} (\overline{FC})$$

$$(\overline{FC}) = \frac{1}{Q_A} \sum_v \sum_w \exp\left(\frac{-\epsilon_{Av}}{RT}\right) S_{Av,Bw}^2 \delta(\epsilon_{Av} - \epsilon_{Bw}) \tag{2}$$

$$Q_A = \sum_v \exp\left(\frac{-\epsilon_{Av}}{RT}\right)$$

where $(\overline{FC})$ is a thermally averaged Franck–Condon (vibrational overlap) factor. Equation (2) is a general expression for the probability of a transition from an initial electronic state A to a final electronic state B. It is valid provided that the density of final states is large and the transition probability small.

In the systems considered here the electronic transition involves electron transfer between two redox sites (a donor, D, and an acceptor, A).

$$\underset{\substack{\text{initial state}\\ A}}{\mathrm{D}\cdots\mathrm{A}} \xrightarrow{k} \underset{\substack{\text{final state}\\ B}}{\mathrm{D}^{+}\cdots\mathrm{A}^{-}} \tag{3}$$

Subject to the constraints discussed above, the (first-order) rate constant for the electron transfer is given by Eq. (2). Evidently the rate constant depends upon the magnitude of the electronic coupling between the initial and final states and on the value of the thermally averaged Franck–Condon factor. In this Comment we present expressions for the Franck–Condon factor for various situations.

For electron-transfer reactions of metal complexes three broad classes of vibrational modes need to be considered: the high-frequency (fast) modes ($\hbar\omega_f > 1000\ \mathrm{cm}^{-1}$) which are mainly the intraligand vibrations, the intermediate (complex) modes ($1000 > \hbar\omega_c > 100\ \mathrm{cm}^{-1}$) that typically include the metal-ligand stretching vibrations, and the low-frequency (slow) modes ($\hbar\omega_s < 100\ \mathrm{cm}^{-1}$) which are primarily the orientational and librational motions of the solvent. At ordinary temperatures $\hbar\omega_f >> kT \sim \hbar\omega_c >> \hbar\omega_s$. This allows the low-frequency modes to be treated using classical continuum expressions. We further assume that the intramolecular vibrations are harmonic with identical force constants. Although the frequency of a particular intramolecular vibration generally changes with oxidation state, the energy surfaces for the reaction can be "symmetrized" by using a reduced frequency (averaged over the two oxidation states) for each vibration. The error introduced by this approximation is quite small in most instances.[10] Because of the use of symmetrized energy surfaces, only intramolecular modes which undergo a net displacement (i.e., for which there is a change in equilibrium nuclear configuration in the two oxidation states) contribute to the Franck–Condon factors.[15a]

We shall denote the mode displacement by the reduced reorganization parameter $S_j = \Delta_j^2/2$ where Δ_j is the reduced displacement of the initial- and final-state equilibrium configurations along

the jth normal coordinate ($\Delta_j^2 = f_j(\Delta Q^\circ_j)^2/\hbar\omega_j$, $S_j = \lambda_j/\hbar\omega_j$ is the reorganization paramater in quanta, f_j is the force constant, ω_j is the angular frequency, ΔQ°_j is the equilibrium displacement, and λ_j is the (vertical) reorganization parameter for the jth mode). Finally, we define ΔE for the reaction as the energy of the final state minus that of the initial state (Fig. 1)[15b] and we draw attention to the need to distinguish between energies (enthalpies) and free energies.[15c]

I. SINGLE-MODE EXPRESSIONS

We first consider the case in which only a single vibrational mode of angular frequency ω undergoes displacement in the electron-

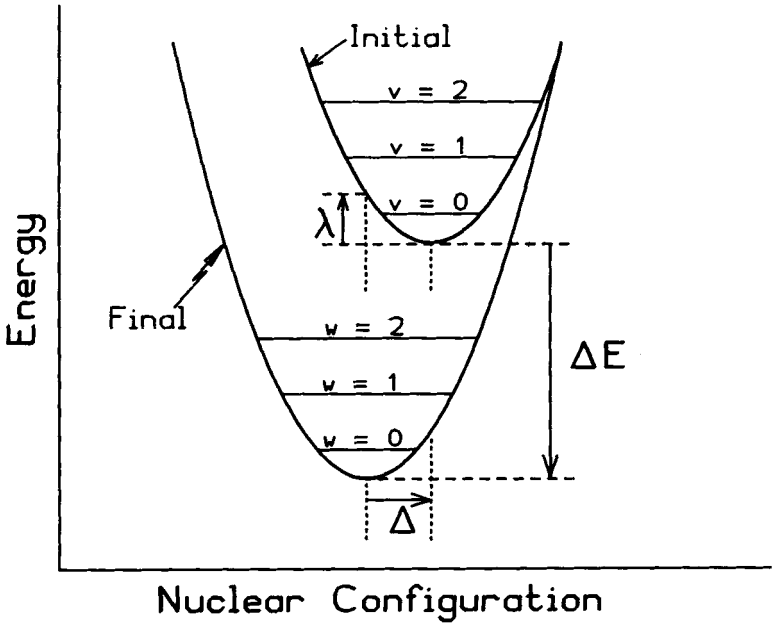

FIGURE 1 Potential energy surfaces for the initial (upper curve) and final (lower curve) states of an electron-transfer reaction. Δ is the reduced displacement of the initial- and final-state equilibrium configurations along a normal coordinate; ΔE is the energy of the final state minus that of the initial state (negative for a spontaneous reaction) and λ is the reorganization parameter.

transfer process. In order that energy be conserved in the electron transfer only those transitions are allowed in which the vibrational quantum number increases from v in the initial state to $v + |\Delta E|/\hbar\omega$ in the final state, where $|\Delta E|$ is the energy released in the reaction. The increase in vibrational energy is thus equal to the decrease in electronic energy resulting from the electron transfer. Under these conditions the rate constant for the electron transfer is given by[11]

$$k = \frac{2\pi H_{AB}^2}{\hbar^2\omega} \exp[-S(2\bar{n} + 1)][(\bar{n} + 1)/\bar{n}]^{m/2} \times I_m\{2S[\bar{n}(\bar{n} + 1)]^{1/2}\} \tag{4a}$$

or, in terms of hyperbolic functions, by

$$k = \frac{2\pi H_{AB}^2}{\hbar^2\omega} \exp\left[-S \coth\left(\frac{\hbar\omega}{2kT}\right)\right] \exp\left(\frac{|\Delta E|}{2kT}\right) \times I_m\left\{S \operatorname{csch}\left(\frac{\hbar\omega}{2kT}\right)\right\} \tag{4b}$$

where $m = |\Delta E|/\hbar\omega$, $\bar{n}$ is the average quantum number of identical oscillators in thermal equilibrium at temperature T, $I_m(z)$ is the modified Bessel function[16] of order m

$$\bar{n} = \frac{1}{e^{\hbar\omega/kT} - 1} \tag{5a}$$

$$I_m(z) = \left(\frac{z}{2}\right)^m \sum_{k=0}^{\infty} \frac{(z^2/4)^k}{k!(m + k)!} \tag{5b}$$

and $z = 2S[\bar{n}(\bar{n} + 1)]^{1/2} = S \operatorname{csch}(\hbar\omega/2kT)$. If the system literally has only a single active vibrational mode, the rate constant will be equal to zero for nonintegral values of m, i.e., for certain values of ΔE. In practice, however, there will always be additional vibrational modes that allow the transition to occur at $|\Delta E| \approx m\hbar\omega$. As a consequence, m is generally taken as the integer closest in

value to $|\Delta E|/\hbar\omega$. When the spacing ($\hbar\omega$) between the vibrational levels is large, then resonance or "quantum beat" effects may appear, with the value of the rate constant being very small for certain ΔE values.

Two limiting forms of the Bessel function (Eq. (5b)) are of interest. When z is small (low T, small S; $kT << \hbar\omega/2$) the sum can be approximated by the first ($k = 0$) term,

$$I_m(z) \rightarrow \left(\frac{z}{2}\right)^m \Big/ m! \tag{5c}$$

while, when z is large (high T, large S; $(4\lambda RT)^{1/2} >> |\Delta E| >> \hbar\omega$),[16]

$$I_m(z) \rightarrow \frac{1}{(2\pi z)^{1/2}} \exp\left(z - \frac{m^2}{2z}\right) \tag{5d}$$

Using these limiting forms the following expressions are obtained for the electron-transfer rate constant in the low- and high-temperature limits.

Ia. *Low-temperature limit: $\hbar\omega >> kT$.*

The low-temperature limit of Eq. (4) is

$$k = \frac{2\pi H_{AB}^2}{\hbar^2\omega} \exp(-S) \frac{S^m}{m!} \tag{6a}$$

$$= \frac{H_{AB}^2}{\hbar} \left(\frac{2\pi}{\hbar\omega|\Delta E|}\right)^{1/2} \exp(-S - \gamma_0 m) \tag{6b}$$

where $\gamma_0 = \ln(m/S) - 1 = \ln(|\Delta E|/\lambda) - 1$. In this case the rate constant is independent of temperature: the reaction occurs from the $v = 0$ vibrational level of the initial state to the $v' = |\Delta E|/\hbar\omega$ level of the final state. In deriving Eq. (6b) we have used an approximation based on Stirling's formula.[17a]

Ib. *High-temperature limit:* $\hbar\omega << kT$.

Noting that, at high temperatures,[17b]

$$2S[\bar{n}(\bar{n} + 1)]^{1/2} - S(2\bar{n} + 1) \rightarrow - \frac{S\hbar\omega}{4kT}$$

and that $\lambda = S\hbar\omega$, leads to the high-temperature (classical) limit of Eq. (4)

$$k = \frac{H_{AB}^2}{\hbar}\left(\frac{\pi}{\lambda RT}\right)^{1/2} \exp\left[-\frac{(\Delta E + \lambda)^2}{4\lambda RT}\right] \tag{6c}$$

This limit corresponds to an activated barrier-crossing reaction. Equation (6c) is also readily derivable from transition-state theory using a Landau–Zener treatment of the barrier crossing in the weak-interaction limit.[2,14]

Ic. *Closed-form expression.*

By expressing the rate as a product of three factors, namely, the rate at which the system approaches the barrier, the tunneling probability and a Landau–Zener type factor, and using a saddle-point approximation Scher and Holstein[18] derived the following expression for the rate constant for the single-mode case:

$$k = \frac{H_{AB}^2}{\hbar}\left(\frac{2\pi}{\lambda\hbar\omega[\Delta E^2/\lambda^2 + \operatorname{csch}^2(\hbar\omega/2kT)]^{1/2}}\right)^{1/2} \times \exp\left(-\frac{\Delta E}{2RT} - \frac{\lambda}{\hbar\omega}\left\{\coth\left(\frac{\hbar\omega}{2kT}\right) - \left[\frac{\Delta E^2}{\lambda} + \operatorname{csch}^2\left(\frac{\hbar\omega}{2kT}\right)\right]^{1/2} + \left(\frac{\Delta E}{\lambda}\right)\sinh^{-1}\left[\left(\frac{\Delta E}{\lambda}\right)\sinh\left(\frac{\hbar\omega}{2kT}\right)\right]\right\}\right) \tag{7}$$

The above expression is a very good approximation to Eq. (4b) at all temperatures even when $\hbar\omega >> 2kT$.

II. TWO-MODE EXPRESSIONS

In this section we consider the case where two vibrational modes, one of low frequency (ω_s) and the other of high frequency (ω_f), undergo displacement. Provided that the two frequencies are sufficiently different, the rate constant for this case is given by[9,11]

$$k = \frac{2\pi H_{AB}^2}{\hbar^2 \omega_s} \exp\left[-S_s \coth\left(\frac{\hbar\omega_s}{2kT}\right) - S_f \coth\left(\frac{\hbar\omega_f}{2kT}\right) \right]$$

$$\times \sum_{p(m)=-\infty}^{+\infty} \sum_{m=-\infty}^{+\infty} \exp\left[\frac{p(m)\hbar\omega_s}{2kT}\right] I_{|p(m)|}\left\{ S_s \operatorname{csch}\left(\frac{\hbar\omega_s}{2kT}\right)\right\} \quad (8)$$

$$\times \exp\left(\frac{m\hbar\omega_f}{2kT}\right) I_{|m|}\left\{ S_f \operatorname{csch}\left(\frac{\hbar\omega_f}{2kT}\right)\right\}$$

where m is the change in quantum number for the high-frequency mode, $\Delta\epsilon = m\hbar\omega_f$, and $p(m) = [|\Delta E| - \Delta\epsilon]/\hbar\omega_s$. Evidently the effective driving force for the reorganization of the low-frequency mode is the original electronic energy gap (positive) minus the increase in the vibrational energy of the high-frequency mode. Because of the presence of the low-frequency mode, exact energy equality between $|\Delta E|$ and $m\hbar\omega$ is no longer required.

IIa. *Low-frequency mode is in the high-temperature limit: $\hbar\omega_s << kT$.*

In this case the low-frequency mode can be treated classically. At high temperatures the Bessel function for the low-frequency mode becomes

$$I_{p(m)}(z) \rightarrow \frac{1}{(4\pi S_s kT/\hbar\omega_s)^{1/2}} \exp\left[S_s \operatorname{csch}\left(\frac{\hbar\omega_s}{2kT}\right) - \frac{\{(|\Delta E| - m\hbar\omega_f)/\hbar\omega_s\}^2}{4S_s kT/\hbar\omega_s} \right]$$

and the rate constant is given by

$$k = \frac{H_{AB}^2}{\hbar}\left(\frac{\pi}{\lambda_s RT}\right)^{1/2} \exp\left[-S_f \coth\left(\frac{\hbar\omega_f}{2kT}\right)\right]$$
$$\times \sum_{m=-\infty}^{+\infty} \exp\left(\frac{m\hbar\omega_f}{2kT}\right) I_{|m|}\left\{S_f \operatorname{csch}\left(\frac{\hbar\omega_f}{2kT}\right)\right\} \tag{9}$$
$$\times \exp\left[-\frac{(\Delta E + m\hbar\omega_f + \lambda_s)^2}{4\lambda_s RT}\right]$$

Equation (9) is a generalization of Eq. (4b) where the delta function (that ensures that $m = |\Delta E|/\hbar\omega$; see also Eq. (2)) has been replaced by a Gaussian. The low-frequency modes now accept (or provide) the difference in energy between $|\Delta E|$ and $m\hbar\omega_f + \lambda_s$, thereby reducing the need for exact equivalence between these two quantities. However, since the Gaussian is strongly peaked at $m = (|\Delta E| - \lambda_s)/\hbar\omega_f$, the terms near this maximum will dominate the sum.

IIb. *Low-frequency mode is in the high-temperature limit; high-frequency mode is in the low-temperature limit:* $\hbar\omega_s << kT << \hbar\omega_f$.

This is an important case and will be discussed in some detail. When the high-frequency mode is in the low-temperature limit all of the reaction occurs from the lowest vibrational level of the high-frequency mode. This restricts the sum over m to positive values. Substituting the low-temperature form for the Bessel function gives

$$k = \frac{H_{AB}^2}{\hbar}\left(\frac{\pi}{\lambda_s RT}\right)^{1/2} \exp(-S_f) \sum_{m=0}^{\infty} \frac{S_f^m}{m!}$$
$$\times \exp\left[-\frac{(\Delta E + m\hbar\omega_f + \lambda_s)^2}{4\lambda_s RT}\right] \tag{10a}$$

The thermally averaged Franck–Condon factor for this case is (see

Eq. (2))

$$(\overline{FC}) = \frac{\exp(-S_f)}{(4\pi\lambda_s RT)^{1/2}} \sum_{m=0}^{\infty} \frac{S_f^m}{m!} \exp\left[- \frac{(\Delta E + m\hbar\omega_f + \lambda_s)^2}{4\lambda_s RT} \right] \quad (10b)$$

The effects of temperature and driving force on the thermally averaged Franck–Condon factors (Eq. (10b)) are shown in Fig. 2. In the normal free-energy region ($|\Delta E| < \Sigma\lambda_j$) the $\overline{FC}$ factor increases with increasing temperature. In this region the classical nuclear reorganization barrier is "wide" and nuclear tunneling corrections to the classical expressions are small. As a consequence the rate constants have only a weak dependence on $\hbar\omega_f$ (at constant λ_f). By contrast, the nuclear tunneling corrections are large in the inverted free-energy region ($|\Delta E| > \Sigma\lambda_j$) particularly when $\hbar\omega_f >$

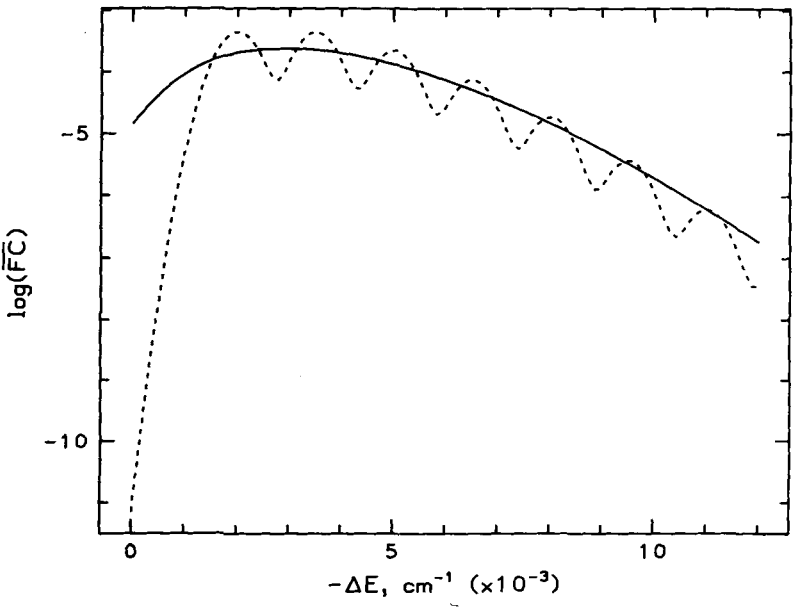

FIGURE 2 Plot of the logarithm of the thermally averaged Franck–Condon factors vs. the driving force for the reaction for the two-mode case. The exact factors are calculated using Eq. (10b). The solid and dotted curves are for T = 298 K and 40 K, respectively. The calculations assume λ_s = 2000 cm^{-1}, λ_f = 1500 cm^{-1} and $\hbar\omega_f$ = 1500 cm^{-1}.

$2kT$. The rate constants in the inverted region are almost independent of temperature and are much less sensitive to the driving force for electron transfer than are the rate constants in the normal region. Further, the decrease of $\overline{FC}$ with increasing driving force in the inverted region is controlled by $\hbar\omega_f$ in addition to λ_f:[17c] an increase in either results in an increase in $\overline{FC}$ at a given temperature. Note the "quantum beats" in the inverted region at low temperature.

A convenient closed-form expression for the rate constant can be derived as follows. The sum in Eq. (10a) is replaced by an integral over m, and the integrand is treated as a Gaussian with a maximum occurring at $m = m^*$.[19] The thermally averaged Franck–Condon factor is then equal to the area under the Gaussian-type curve: the area under this curve is approximated by the product of three factors, namely, the maximum value of the integrand, its $1/e$ width in vibrational quanta (we approximate the width by $4(\lambda_s RT)^{1/2}/\hbar\omega_f$), and a normalization factor ($(\pi/4)^{1/2}$). This procedure gives[19]

$$k \approx \frac{2\pi H_{AB}^2}{\hbar} \frac{\exp(-S_f)}{\hbar\omega_f} \frac{S_f^{m^*}}{m^*!} \exp\left[-\frac{(\Delta E + m^*\hbar\omega_f + \lambda_s)^2}{4\lambda_s RT}\right] \quad (10c)$$

where

$$m^* \approx \frac{|\Delta E| - \lambda_s}{\hbar\omega_f} - \frac{2\lambda_s RT(\gamma + 1)}{(\hbar\omega_f)^2} \quad (10d)$$

and

$$\gamma = \ln[(|\Delta E| - \lambda_s)/\lambda_f] - 1$$

Within this approximation most of the reaction at low temperature occurs from the $v = 0$ to the $v = m^*$ level of the high-frequency mode. In effect the low-frequency mode reduces the driving force (energy gap) from $|\Delta E|$ to $|\Delta E| - \lambda_s$ and the dominant high-frequency vibrational transition at low temperature is no longer from $v = 0 \rightarrow v' = |\Delta E|/\hbar\omega_f$ as it was in the absence of the low-frequency mode.

Substituting for m^* in Eq. (10c) and using Stirling's approximation gives

$$k \approx \frac{H_{AB}^2}{\hbar}\left(\frac{2\pi}{\hbar\omega_f(|\Delta E| - \lambda_s)}\right)^{1/2} \times \exp\left[-\frac{\lambda_f}{\hbar\omega_f} - \frac{\gamma(|\Delta E| - \lambda_s)}{\hbar\omega_f} + \left(\frac{\gamma + 1}{\hbar\omega_f}\right)^2 \lambda_s RT\right] \quad (11)$$

Note that, in contrast to Eqs. (10c) and (10d), which are valid in both the normal and inverted free-energy regions, Eq. (11) is valid only in the inverted region.[20a] Note also that the temperature dependence of the rate constant arises from the third term in the exponent of Eq. (11).[20b]

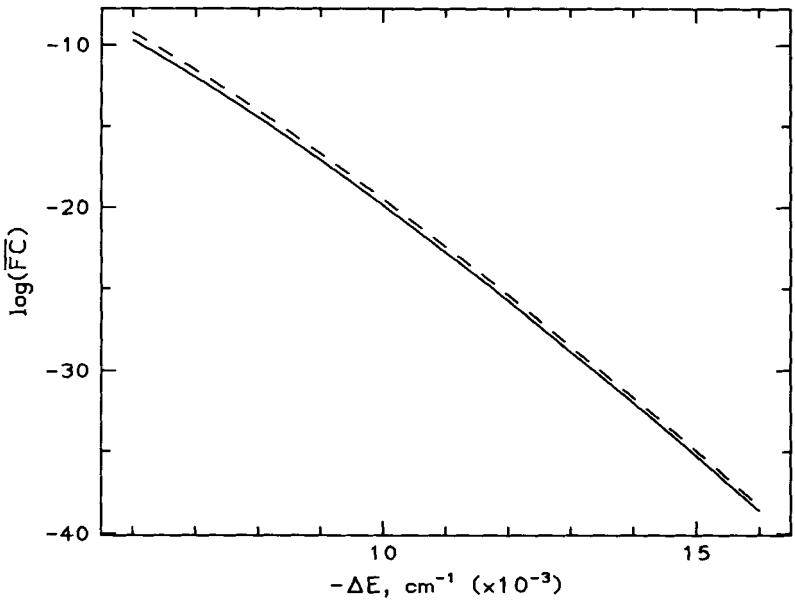

FIGURE 3 Plot of the logarithm of the thermally averaged Franck–Condon factors vs. the driving force for the reaction for the two-mode case. The exact factors (Eq. (10b), solid curve) are compared with those given by analytical approximation (Eq. (11), dashed curve). The curve calculated using Eqs. (10c–d) is indistinguishable from the solid curve. The calculations assume $\lambda_s = 1000\ cm^{-1}$, $\lambda_f = 250\ cm^{-1}$, $\hbar\omega_f = 500\ cm^{-1}$ and $T = 298$ K.

The thermally averaged Franck–Condon factors calculated with the above equations are compared in Figs. 3–5. Equations (10c) and (10d) yield thermally averaged Franck–Condon factors that are within 20% of those given by Eq. (10b) provided that the width of the Gaussian is larger than one vibrational quantum, i.e., $W_G = 4(\lambda_s RT)^{1/2}/\hbar\omega_f \geq 1$. Vibronic structure or "quantum beat" effects can become very important when this condition is not satisfied: such effects are not allowed for in the approximation used to derive Eqs. (10c) and (10d). Thus when $W_G \approx 0.3 - 0.5$ and $m^* = n + 1/2$, where n is an integer, $\overline{FC}$ calculated with Eqs. (10c) and (10d) can be more then an order of magnitude too large, while, when m^* is an integer, Eqs. (10c) and (10d) yield $\overline{FC}$ values that are too small (Fig. 5). Although the amplitude of the quantum beats decrease with increasing temperature, quantum beat effects

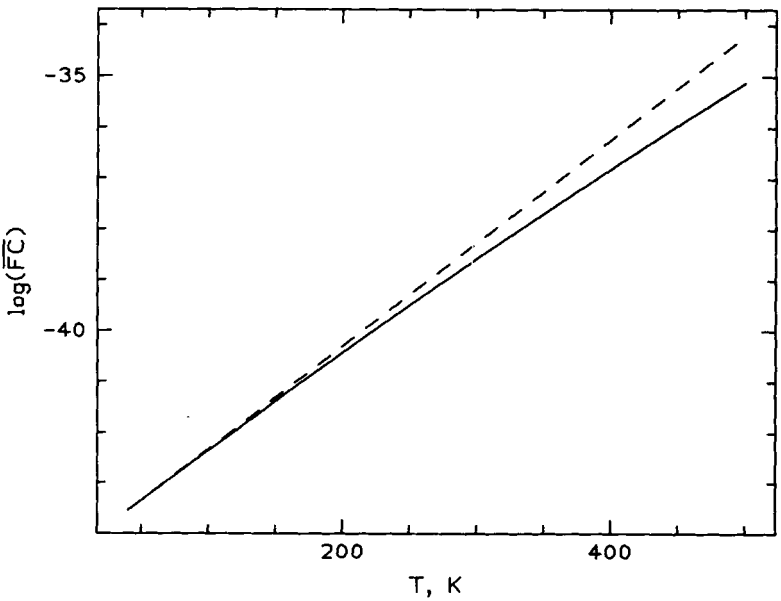

FIGURE 4 Plot of the logarithm of the thermally averaged Franck–Condon factors vs. temperature for the two-mode case. The exact factors (Eq. (10b), solid curve) are compared with those given by the analytical approximation (Eq. (11), dashed curve). The curve calculated using Eqs. (10c–d) is indistinguishable from the solid curve. The calculations assume $\Delta E = -16000\ cm^{-1}$, $\lambda_s = 1000\ cm^{-1}$, $\lambda_f = 250\ cm^{-1}$ and $\hbar\omega_f = 500\ cm^{-1}$.

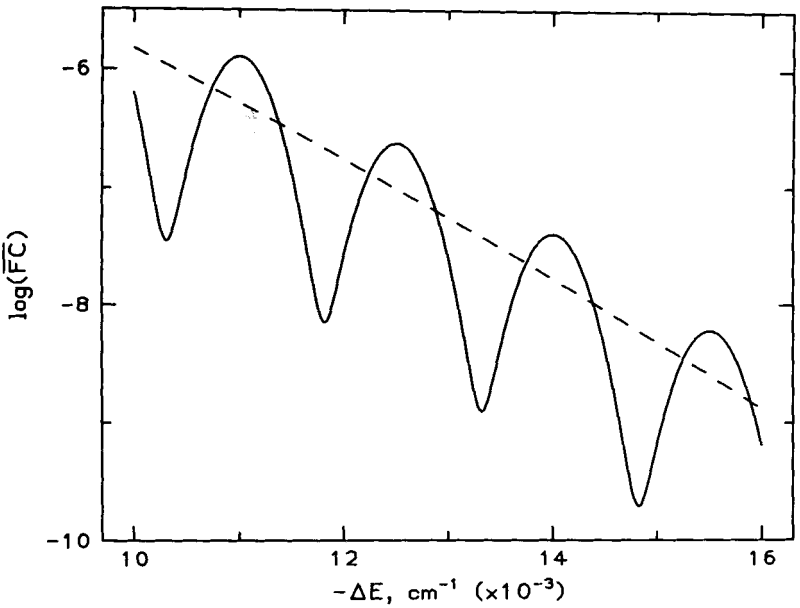

FIGURE 5 Plot of the logarithm of the thermally averaged Franck–Condon factors vs. the driving force for the reaction for the two-mode case. Note that the oscillatory character (quantum beats) of the exact factors (Eq. (10b), solid curve) is not reproduced by the analytical approximation (Eq. (11), dashed curve). The curve calculated using Eqs. (10c–d) is indistinguishable from the dashed curve. The calculations assume $\lambda_s = 500\ \text{cm}^{-1}$, $\lambda_f = 2250\ \text{cm}^{-1}$, $\hbar\omega_f = 1500\ \text{cm}^{-1}$ and $T = 80$ K.

can be important even at room temperature. Note, however, that other factors can also reduce the rate oscillations (see the three-mode section below).

A closed-form expression that is very similar to Eq. (11), but somewhat less accurate, can be derived starting with the low-temperature limit (see Appendix).

IIc. *Both the high-frequency and the low-frequency modes are in the high-temperature limit:* $\hbar\omega_s << \hbar\omega_f << kT$.

The high-temperature limit of Eq. (9) is obtained by first taking the Bessel function to its high-temperature limit. This procedure

gives

$$k = \frac{\omega_f H_{AB}^2}{2(\lambda_f \lambda_s)^{1/2} RT}$$

$$\times \sum_{m=-\infty}^{+\infty} \exp\left[- \frac{(m\hbar\omega_f - \lambda_f)^2}{4\lambda_f RT} - \frac{(\Delta E + m\hbar\omega_f + \lambda_s)^2}{4\lambda_s RT} \right] \quad (12a)$$

where $\lambda_f = S_f \hbar\omega_f$. Next the sum is evaluated in the high-temperature limit. Recalling that $\Delta\epsilon = m\hbar\omega_f$ the summation may be replaced by integration to give

$$k = \frac{H_{AB}^2}{\hbar} \left(\frac{\pi}{(\lambda_s + \lambda_f) RT} \right)^{1/2} \exp\left[- \frac{(\Delta E + \lambda_s + \lambda_f)^2}{4(\lambda_s + \lambda_f) RT} \right] \quad (12b)$$

which is the classical activated-complex expression for the two-mode case.

III. THREE-MODE EXPRESSIONS

In this section we present the rate constant for the case where three vibrational modes need to be considered, one of low frequency (ω_s), a second of intermediate frequency (ω_c) and a third of high frequency (ω_f).

IIIa. *High-frequency mode is in the low-temperature limit, and the low-frequency mode is in the high-temperature limit:* $\hbar\omega_s << kT \sim \hbar\omega_c << \hbar\omega_f$.

When the low-frequency mode is treated classically the rate constant is given by

$$k = \frac{H_{AB}^2}{\hbar} \left(\frac{\pi}{\lambda_s RT} \right)^{1/2} \exp\left[-S_f - S_c \coth\left(\frac{\hbar\omega_c}{2kT} \right) \right]$$

$$\times \sum_{m_f=0}^{\infty} \sum_{m_c=-\infty}^{\infty} \frac{S_f^{m_f}}{m_f!} \exp\left(\frac{m_c \hbar\omega_c}{2kT} \right) I_{m_c}\left\{ S_c \operatorname{csch}\left(\frac{\hbar\omega_c}{2kT} \right) \right\}$$

$$\times \exp\left[- \frac{(\Delta E + m_f \hbar\omega_f + m_c \hbar\omega_c + \lambda_s)^2}{4\lambda_s RT} \right] \quad (13a)$$

where m_f and m_c are the changes in the vibrational quantum numbers of the high- and intermediate-frequency modes, respectively.[21a] Using Eq. (A2) and proceeding as in the derivation of the two-mode Eqs. (A3)–(A6), the following closed-form expression can be derived for the three-mode case for reactions in the *inverted region*[21b]

$$k \approx \frac{2H_{AB}^2}{\hbar}\left[\frac{\pi}{2\hbar\omega_f(|\Delta E| - (\lambda_c + \lambda_s))}\right]^{1/2}$$

$$\times \exp\left\{-\frac{\lambda_f}{\hbar\omega_f} - \frac{(\gamma_0 + 1)(\lambda_c + \lambda_s)}{\hbar\omega_f} - \frac{\gamma_0|\Delta E|}{\hbar\omega_f}\right.$$

$$\left. + \frac{(\gamma_0 + 1)^2}{(\hbar\omega_f)}\left[\lambda_s RT + \frac{\lambda_c\hbar\omega_c}{2}\coth\left(\frac{\hbar\omega_c}{2kT}\right)\right]\right\} \qquad (13b)$$

where $\gamma_0 = [\ln(|\Delta E|/\lambda_f) - 1] \approx \gamma + \lambda_s/|\Delta E|$. The rate constants calculated with Eq. (13b) are in excellent agreement with those calculated with Eq. (13a) provided that $\hbar\omega_f > 2.5\ \hbar\omega_c$ and $5\lambda_c$ and $10\lambda_s$ are each $\leq|\Delta E|$.

Comparisons of the thermally averaged Franck–Condon factors calculated from Eqs. (13a) and (13b) are presented in Figs. 6 and 7. The effect of an intermediate vibrational frequency can be seen by comparing Fig. 4 with Fig. 6 where the same λ_s, λ_f, $\hbar\omega_f$ and T values and $|\Delta E|$ range have been used: only an intermediate mode of 500 cm^{-1} frequency with a very small reorganization energy (λ_c = 100 cm^{-1}, S_c = 0.2) has been introduced. The addition of this intermediate mode reduces the amplitude of the quantum beats. A small increase in the reduced displacement of the intermediate mode (λ_c = 250 cm^{-1}, S_c = 0.5) almost completely obliterates the quantum beat effect (Fig. 7): at higher temperature the loss of quantum beats occurs for even smaller values of λ_c. The experimental observation of quantum beats is thus unlikely for metal complexes that have intermediate metal–ligand frequencies with even modest displacements.

Calculations show that the maximal contribution to the rate

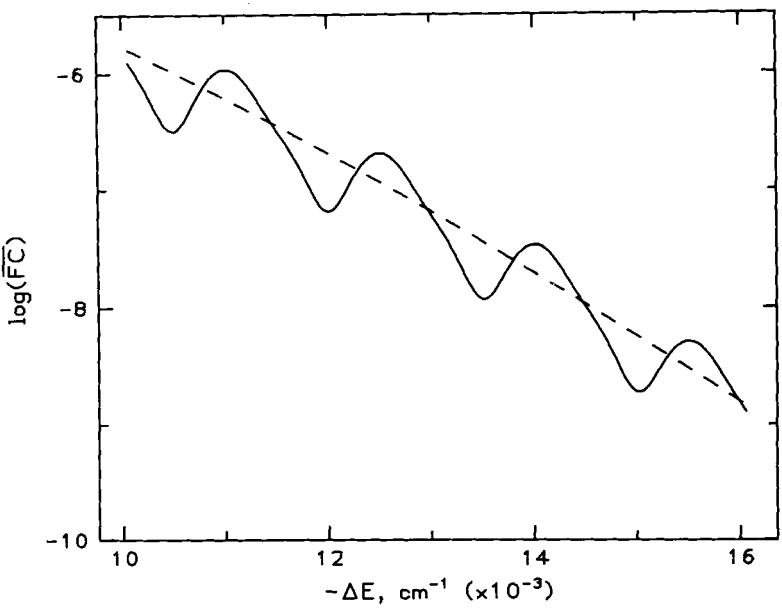

FIGURE 6 Plot of the logarithm of the thermally averaged Franck–Condon factors vs. the driving force for the reaction for the three-mode case. The exact factors (Eq. (13a), solid curve) are compared with the analytical approximation (Eq. (13b), dashed curve). The calculations assume $\lambda_s = 500\ \text{cm}^{-1}$, $\lambda_c = 100\ \text{cm}^{-1}$, $\hbar\omega_c = 500\ \text{cm}^{-1}$, $\lambda_f = 2250\ \text{cm}^{-1}$, $\hbar\omega_f = 1500\ \text{cm}^{-1}$ and $T = 80$ K.

occurs for the $m_f = 0$ to $m_f = m_f^*$ and $m_c = 0$ to $m_c = m_c^*$ transitions where

$$m_f^*\hbar\omega_f + m_c^*\hbar\omega_c \approx |\Delta E| - \lambda_s - \frac{2\lambda_s RT(\gamma + 1)}{\hbar\omega_f}$$

and

$$\frac{m_f^* - S_f}{m_c^* - S_c} \approx \frac{\lambda_f\hbar\omega_f}{\lambda_c\hbar\omega_c}$$

The second expression is only very approximate due to the quantum nature of the modes. These expressions require that when $\lambda_f/\lambda_c \gtrsim 1$ most of the excess energy is acquired by the high-energy

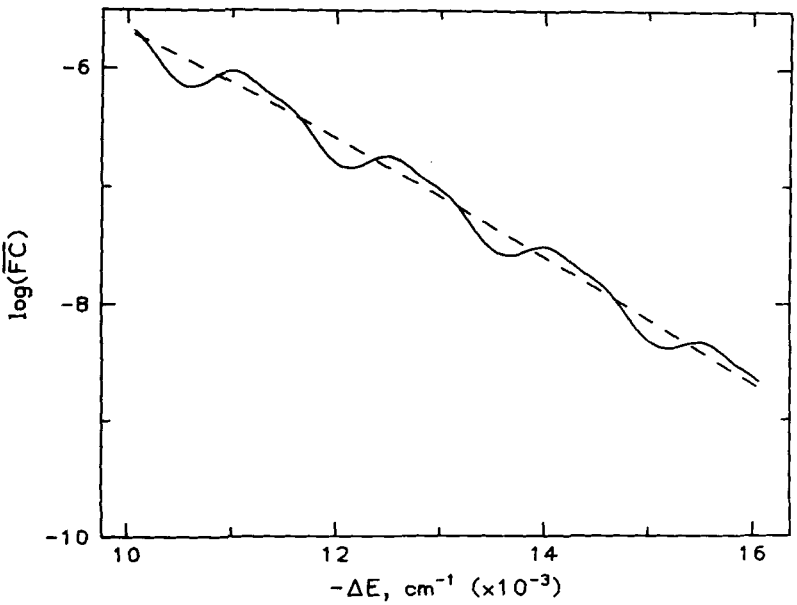

FIGURE 7 Plot of the logarithm of the thermally averaged Franck–Condon factors vs. the driving force for the reaction for the three-mode case. The exact factors (Eq. (13a), solid curve) are compared with the analytical approximation (Eq. (13b), dashed curve). The calculations assume $\lambda_s = 500\ cm^{-1}$, $\lambda_c = 250\ cm^{-1}$, $\hbar\omega_c = 500\ cm^{-1}$, $\lambda_f = 2250\ cm^{-1}$, $\hbar\omega_f = 1500\ cm^{-1}$ and $T = 80$ K.

mode:[17c] the intermediate-frequency mode receives an amount less than one high-frequency vibrational quantum. Only when $\lambda_f/\lambda_c \leq 0.1$ does the amount of energy deposited in the intermediate frequency mode becomes significant. For example, $m_c^* = 11$ and $m_f^* = 8$ when $\lambda_f = 100\ cm^{-1}$, $\hbar\omega_f = 1350\ cm^{-1}$, $\lambda_c = 1000\ cm^{-1}$, $\hbar\omega_c = 350\ cm^{-1}$, $\lambda_s = 1000\ cm^{-1}$, $T = 298$ K, and $\Delta E = -17{,}000\ cm^{-1}$. This results in 10,700 cm^{-1} of excess energy ($8 \times 1350 - 100$) in the high-frequency mode and only 2,850 cm^{-1} of excess energy ($11 \times 350 - 1000$) in the intermediate-frequency mode. This energy distribution also reflects the effect of adding a high-frequency mode on the rate of the reaction. Figure 8 shows that, while the rate change due to the addition of a high-frequency mode is modest in the normal free-energy region, it is dramatic in the inverted region.[21c] This accounts for the relative unimportance of

small-displacement high-frequency modes on the rates of electron-transfer reactions of metal complexes in solution: such reactions are usually in the normal region. By contrast, the nonradiative decay rates of charge-transfer excited states for many metal-complexes are in the inverted region and here the high-frequency modes have a dominant effect on the decay rates.

The contributions of the individual terms in Eq. (13a) to the rate constant are illustrated in Figs. 9(a) and 9(b) for a typical electron-transfer reaction in the inverted region. It is evident that relatively few terms contribute to the Franck–Condon sum and that the values of the individual terms are much more steeply peaked along the high-frequency direction than along the intermediate-frequency direction. The ridge line is seen in Fig. 9(a) to run at an angle to the axes.

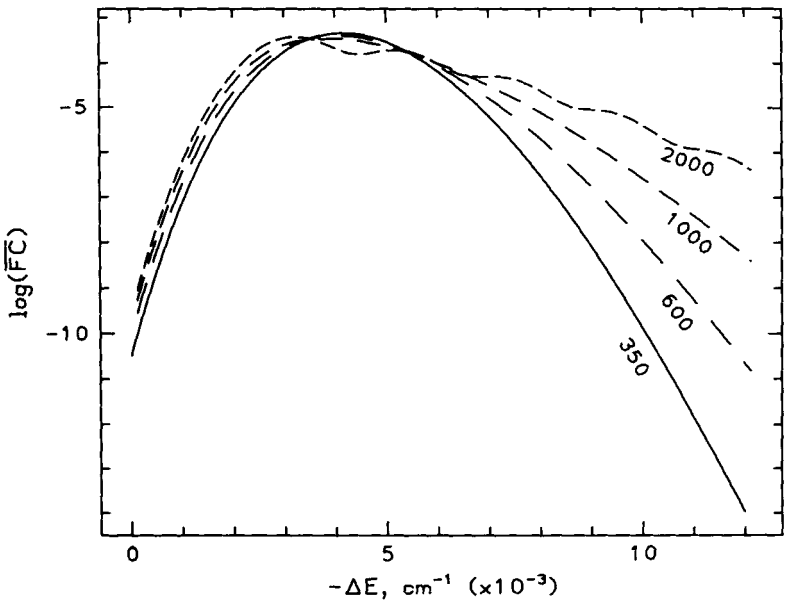

FIGURE 8 Plot of the logarithm of the thermally averaged Franck–Condon factors vs. the driving force for the three-mode case. The factors are calculated using Eq. (13a) assuming $\lambda_s = 3000\ cm^{-1}$, $\lambda_c = 250\ cm^{-1}$, $\hbar\omega_c = 350\ cm^{-1}$, $\lambda_f = 1000\ cm^{-1}$, $T = 80$ K and $\hbar\omega_f$ values of 350, 600, 1000 and 2000 cm^{-1} as shown.

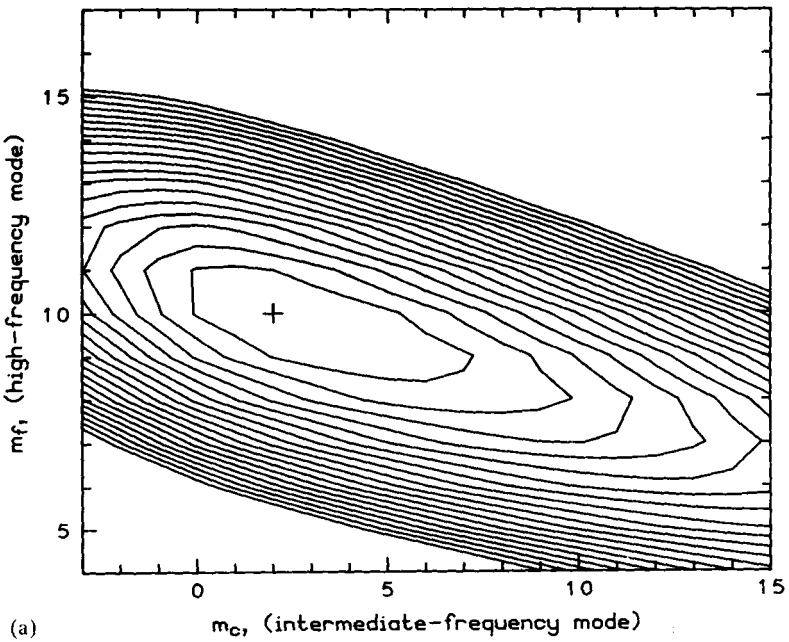

(a)

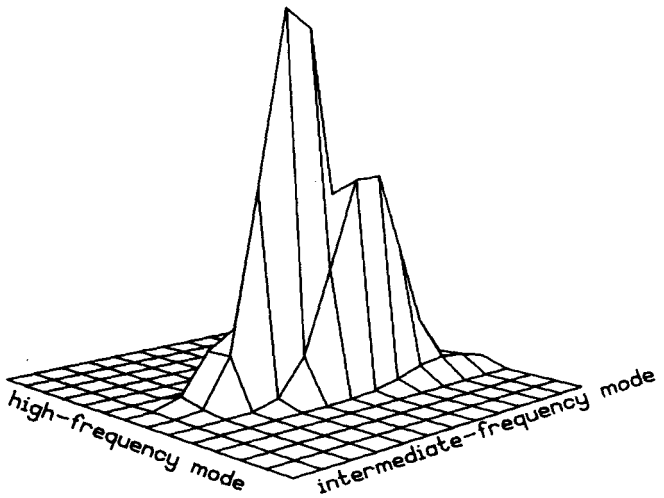

(b)

CONCLUSIONS

In this Comment we have presented expressions for the rate constants for nonadiabatic electron-transfer reactions. More specifically, we have considered reactions where one, two, or three modes undergo displacement as a consequence of the electron transfer. In deriving the expressions for the multimode cases the lowest-frequency mode was assumed to be in the high-temperature limit.

The expressions presented in this Comment are special cases of the general expression, Eq. (14),[22] which is valid when the lowest-frequency mode (ω_s) is in the high-temperature limit.

$$k = \frac{H_{AB}^2}{\hbar}\left(\frac{\pi}{\lambda_s RT}\right)^{1/2} \exp\left[-\sum_{j\neq s} S_j \coth\left(\frac{\hbar\omega_j}{2kT}\right)\right] \times \prod_{j\neq s}\sum_{m_j=-\infty}^{+\infty} \exp\left(\frac{m_j\hbar\omega_j}{2kT}\right) I_{m_j}\left\{S_j \operatorname{csch}\left(\frac{\hbar\omega_j}{2kT}\right)\right\} \times \exp\left[\frac{\left(\Delta E + \sum_{j\neq s} m_j\hbar\omega_j + \lambda_s\right)^2}{4\lambda_s RT}\right] \quad (14)$$

Compact, closed-form approximations to the Franck–Condon sums, which are good approximations when the highest-frequency mode is in the low-temperature limit and quantum beats are absent, are

FIGURE 9 (a) Contour plot of the individual thermally weighted Franck–Condon factors (Ref. 21) vs. the change in the quantum numbers of the intermediate- and high-frequency modes. The contours are drawn so that each contour shows the decrease of the individual Franck–Condon factors by a factor of 10. The "surface" is only defined for integer values of m_c and m_f but is drawn assuming a continuous surface. The calculations assume $\Delta E = -16000\ \text{cm}^{-1}$, $\lambda_s = 1000\ \text{cm}^{-1}$, $\lambda_c = 500\ \text{cm}^{-1}$, $\hbar\omega_c = 350\ \text{cm}^{-1}$, $\lambda_f = 1000\ \text{cm}^{-1}$, $\hbar\omega_f = 1350\ \text{cm}^{-1}$ and $T = 298$ K. The maximum of the surface occurs at $m_c = 2$, $m_f = 10$. (b) A three-dimensional perspective view of the Franck–Condon surface shown in (a) above. The individual lines are for $m_f = 4$ to 17 and $m_c = -3$ to 9. The surface is drawn by connecting values of the individual Franck–Condon factors at integral values of m_c and m_f. Only relatively few of the individual Franck–Condon factors contribute to the total Franck–Condon sum.

also presented in this Comment. When *all* the modes are in the high-temperature limit, the rate constant is given by the classical expression, Eq. (15).[2,19]

$$k = \frac{H_{AB}^2}{\hbar}\left(\frac{\pi}{\sum\lambda_j RT}\right)^{1/2} \exp\left[-\frac{(\Delta E + \sum\lambda_j)^2}{4\sum\lambda_j RT}\right]$$

Nuclear tunneling effects are much larger in the inverted than in the normal region. Consequently the rate constants in the inverted region are dominated by the high-frequency modes, particularly at room temperature and below. When $|\Delta E| >> \Sigma\lambda_j$ and when $\hbar\omega_f > 2kT$ the high-frequency mode affects the rate primarily by increasing the contribution from nuclear tunneling. This has the following consequences: (i) the decrease in rate with increasing $|\Delta E|$ in the inverted region is reduced, (ii) quantum beats can become manifest, and (iii) the effect of temperature on the rate is reduced. In this region the effect of the intermediate-frequency mode (as well as of the solvent modes) is to decrease the amplitude of the quantum beats and to reduce the effective energy gap for the electron transfer. By contrast, in the normal region and when $|\Delta E| < \lambda_s$ the high-frequency mode ($\hbar\omega_f$) has only a modest influence on the rate constant; in addition, quantum beats are generally much less important. Further, the rate constants are dominated by the reorganization energy (rather than by the frequency of the modes) and the rates remain temperature (and ΔE) dependent. The effects of the high and intermediate frequencies are complicated when $|\Delta E| \approx \Sigma\lambda_j$; however, only small changes in the rate with frequency, temperature, or driving force are expected under these conditions.

Expressions of the type considered here are finding increasing application in the description of a variety of electron-transfer processes, ranging from excited-state decays[12,13] and spin-transitions[23] to electron-transfer reactions of metal complexes[9,14] and metalloproteins.[1,2,11,24] Further applications can be anticipated as additional spectral and structural studies provide much needed information regarding the frequencies (and frequency changes) and the structural changes associated with the electron transfer.

APPENDIX

Freed and Jortner[25] have derived expressions for the rate constant when both $\hbar\omega_f$ and $\Sigma\lambda_j$ are much less than $|\Delta E|$ and *all* the modes are in the low-temperature limit. It follows from their Eq. (V-15) that the thermally averaged Franck–Condon factor for this case is given by

$$(\overline{FC}) = \frac{1}{\left(2\pi\hbar\omega_f|\Delta E_k|\left[1 - \sum_{j\neq f}\Omega_j(1 - \omega_j/\omega_f)\right]\right)^{1/2}} \times \exp\left[-\sum_j S_j - \frac{\gamma_k|\Delta E_k|}{\hbar\omega_f}\right] \quad \text{(A1)}$$

where

$$|\Delta E_k| = |\Delta E| - \hbar\omega_k$$

$$\gamma_k = \ln\left(\frac{|\Delta E_k|}{\lambda_f}\right) - 1 - \sum_{j\neq f}\Omega_j\left(\frac{\omega_f}{\omega_j}\right)$$

$$\Omega_j = \frac{S_j\omega_j}{S_f\omega_f}\left(\frac{\lambda_f}{|\Delta E_k|}\right)^{1-\omega_j/\omega_f}$$

and subscript k denotes the promoting mode. For the present purpose we will assume that the promoting mode is a metal–ligand vibration of intermediate frequency and neglect $\hbar\omega_k$ compared to $|\Delta E|$. Introducing $\gamma_0 = \ln(|\Delta E|/\lambda_f) - 1$ it follows that

$$\frac{\gamma_k|\Delta E|}{\hbar\omega_f} = \frac{\gamma_0|\Delta E|}{\hbar\omega_f} - \sum_{j\neq f} S_j\left(\frac{|\Delta E|}{\lambda_f}\right)^{\omega_j/\omega_f}$$

so that the thermally averaged Franck–Condon factor for the low-

temperature limit is

$$(\overline{FC}) = \frac{1}{\left(2\pi\hbar\omega_f|\Delta E|\left[1 - \sum_{j\neq f}\Omega_j(1 - \omega_j/\omega_f)\right]\right)^{1/2}} \times \exp\left[-\sum_j S_j - \frac{\gamma_0|\Delta E|}{\hbar\omega_f} - \sum_{j\neq f} S_j\left(\frac{|\Delta E|}{\lambda_f}\right)^{\omega_j/\omega_f}\right] \tag{A2}$$

This approach can be used to derive an expression for the thermally averaged Frank–Condon factor for the two-mode case considered above. For a two-mode system with $\omega_s << \omega_f$ Eq. (A2) gives

$$(\overline{FC}) = \frac{1}{[2\pi\hbar\omega_f(|\Delta E| - \lambda_s)]^{1/2}} \times \exp\left[-S_f - S_s - \frac{\gamma_0|\Delta E|}{\hbar\omega_f} + S_s\left(\frac{|\Delta E|}{\lambda_s}\right)^{\omega_s/\omega_f}\right] \tag{A3}$$

Upon expanding the last term to second order we obtain

$$(\overline{FC}) = \frac{1}{[2\pi\hbar\omega_f(|\Delta E| - \lambda_s)]^{1/2}}\exp\left[-\frac{\lambda_f}{\hbar\omega_f} - \frac{\gamma_0|\Delta E|}{\hbar\omega_f} + (\gamma_0 + 1)\frac{\lambda_s}{\hbar\omega_f} + \left(\frac{\gamma_0 + 1}{\hbar\omega_f}\right)^2\frac{\lambda_s\hbar\omega_s}{2}\right] \tag{A4}$$

Freed and Jortner next introduce temperature dependence through thermal population of the vibrational levels of the low-frequency mode. This is done (their Eq. (IX-10)) by adding to the exponent a term $Z_2(T)$ defined by

$$Z_2(T) = \left(\frac{\gamma_0 + 1}{\hbar\omega_f}\right)^2\lambda_s\hbar\omega_s\bar{n}_s$$

where $\bar{n}_s$ is the average vibrational quantum number of the low-

frequency oscillators. We then obtain

$$(\overline{FC}) = \frac{1}{[2\pi\hbar\omega_f(|\Delta E| - \lambda_s)]^{1/2}} \exp\left[- \frac{\lambda_f}{\hbar\omega_f} - \frac{\gamma_0|\Delta E|}{\hbar\omega_f} + \frac{(\gamma_0 + 1)\lambda_s}{\hbar\omega_f} + \left(\frac{\gamma_0 + 1}{\hbar\omega_f}\right)^2 \frac{\lambda_s\hbar\omega_s}{2} \coth\left(\frac{\hbar\omega_s}{2kT}\right)\right] \quad \text{(A5)}$$

which should be compared with Eq. (11). The preexponential factors for $(\overline{FC})$ are identical. Since $\gamma_0 \approx \gamma + \lambda_s/|\Delta E|$ the temperature-independent terms in the exponents of Eqs. (A5) and (11) are identical provided that a term $-\lambda_s^2/\hbar\omega_f\,|\Delta E|$ in the exponent of Eq. (11) can be neglected. The similarity of the temperature-dependent terms in the exponents becomes apparent when the hyperbolic cotangent in Eq. (A5) is taken to its high-temperature limit.

Acknowledgments

Valuable discussions with Drs. C. Creutz and J. Winkler are gratefully acknowledged. This work was performed at Brookhaven National Laboratory under contract DE-AC02-76-CH00016 with the U.S. Department of Energy and supported by its Division of Chemical Sciences, Office of Basic Energy Sciences.

BRUCE S. BRUNSCHWIG and NORMAN SUTIN
Department of Chemistry,
Brookhaven National Laboratory,
Upton, New York 11973

References

1. D. DeVault, Quart. Rev. Biophys. **13**, 387 (1980).
2. R. A. Marcus and N. Sutin, Biochim. Biophys. Acta **811**, 265 (1985).
3. N. Sutin, *Supramolecular Photochemistry*, ed. V. Balzani (D. Reidel, Dordrecht, Holland, in press).
4. N. S. Hush, M. N. Paddon-Row, E. Cotsaris, H. Oevering, J. W. Verhoeven and M. Heppener, Chem. Phys. Lett. **117**, 8 (1985). J. M. Warman, M. P. de Haas, H. Oevering, J. W. Verhoeven, M. N. Paddon-Row, A. M. Oliver and N. S. Hush, Chem. Phys. Lett. **128**, 95 (1986). N. S. Hush, Coord. Chem. Rev. **64**, 135 (1985).
5. S. S. Isied, A. Vassilian, R. H. Magnuson and H. A. Schwarz, J. Am. Chem. Soc. **107**, 7432 (1986). S. S. Isied, Prog. Inorg. Chem. **32**, 443 (1984). M. R.

Wasielewski, M. P. Niemczyk, W. A. Svec and E. B. Pewitt, J. Am. Chem. Soc. **107**, 1080 (1985). M. R. Wasielewski, M. P. Niemczyk, W. A. Svec and E. B. Pewitt, J. Am. Chem. Soc. **107**, 5562 (1985). S. S. Isied, C. Kuehn and G. Worosila, J. Am. Chem. Soc. **106**, 1722 (1984). R. Bechtold, C. Kuehn, C. Lepre and S. S. Isied, Nature **322**, 286 (1986).
6. P. S. Ho, C. Sutoris, N. Liang, E. Margoliash and B. M. Hoffman, J. Am. Chem. Soc. **107**, 1070 (1985). K. T. Conklin and G. McLendon, Inorg. Chem. **25**, 4084 (1986).
7. J. Winkler, D. G. Nocera, K. M. Yocom, E. Bordignon and H. B. Gray, J. Am. Chem. Soc. **104**, 5782 (1982). D. G. Nocera, J. R. Winkler, K. M. Yocom, E. Bordignon and H. B. Gray, J. Am. Chem. Soc. **106**, 5145 (1984).
8. J. R. Miller and J. W. Beitz, J. Chem. Phys. **74**, 6746 (1981). L. T. Calcaterra, G. L. Closs and J. R. Miller, J. Am. Chem. Soc. **105**, 670 (1983).
9. N. R. Kestner, J. Logan and J. Jortner, J. Phys. Chem. **78**, 2148 (1974). J. Ulstrup and J. Jortner, J. Chem. Phys. **63**, 4358 (1975). J. Ulstrup, *Charge Transfer Processes in Condensed Media* (Springer-Verlag, New York, 1979).
10. B. S. Brunschwig, J. Logan, M. D. Newton and N. Sutin, J. Am. Chem. Soc. **102**, 5798 (1980).
11. J. Jortner, J. Chem. Phys. **64**, 4860 (1976). J. Jortner, J. Am. Chem. Soc. **102**, 6676 (1980).
12. T. J. Meyer, Prog. Inorg. Chem. **30**, 289 (1983).
13. E. M. Kober, J. V. Caspar, R. S. Lumpkin and T. J. Meyer, J. Phys. Chem. **90**, 3722 (1986).
14. N. Sutin, Acc. Chem. Res. **15**, 275 (1982). N. Sutin, Prog. Inorg. Chem. **30**, 441 (1983).
15. (a) Since bond and frequency changes between the oxidized and reduced forms always occur together, no active modes are lost through the symmetrization procedure. (b) Although this definition of ΔE is opposite to that generally used in radiationless decay formalisms, it is the definition used in most other kinetic and thermodynamic treatments. (c) In quantum-mechanical theories it is customary to treat all the intramolecular and solvent nuclear coordinates (excluding the separation of the redox sites) as a collection of independent harmonic oscillators with identical frequencies (or Morse oscillators with identical frequencies and anharmonicities) in the initial and final states. Under these conditions there is no entropy change in the reaction and $\Delta E \sim \Delta G^\circ$. On the other hand, if only the intramolecular coordinates are treated as harmonic or Morse oscillators while the motion of the solvent is treated as classical (with highly anharmonic potential energies which differ in the initial and final states for the individual solvent motions), then λ_s and ΔE are properly interpreted as free-energy changes. See Ref. (2) and R. A. Marcus, J. Chem. Phys. **81**, 4494 (1984).
16. M. Abramowitz and I. A. Stegun (Eds.), Handbook of Mathematical Functions, National Bureau of Standards Applied Mathematics Series No. 55 (1964).
17. (a) This approximation, which is in error by less than 2% for $n > 4$, is

$$\frac{a^n}{n!} = \frac{1}{\sqrt{2\pi n}} \exp\left\{-n\left[\ln\left(\frac{n}{a}\right) - 1\right]\right\}$$

(b) In terms of hyperbolic functions,

$$S \operatorname{csch}\left(\frac{\hbar\omega}{2kT}\right) - S \coth\left(\frac{\hbar\omega}{2kT}\right) \rightarrow -\frac{S\hbar\omega}{4kT}$$

(c) The thermally averaged Franck–Condon factor is sensitive to $\hbar\omega_f$ because the Gaussian factor in Eq. (10b) requires that the main contribution to the sum arise from m values such that $\Delta E + m\hbar\omega_f + \lambda_s \approx 0$. Thus, as $\hbar\omega_f$ increases, the m values that contribute to the sum decrease, the value of $m_f!$ decreases, and $\overline{FC}$ increases. In other words, when $|\Delta E| - \lambda_s$ is large and positive, high-frequency modes that can accept the excess energy in few quanta are highly favored over lower frequency modes. High-frequency modes are therefore good acceptor modes in the inverted region.

18. H. Scher and T. Holstein, Philos. Mag. B **44**, 343 (1981).
19. R. A. Marcus, Faraday Disc. Chem. Soc. **74**, 7 (1982).
20. (a) Because of the neglect of certain terms, use of Eq. (11) requires that $W_G < [1.6(|\Delta E| - \lambda_s)/\hbar\omega_f\,(\gamma + 1)]^{1/2}$. (b) Equation (11) may be compared with Eq. (9) of Ref. 13: the two equations are identical when the group of low-frequency modes ($\Sigma\lambda_i$) in Ref. 13 is replaced by a single low-frequency mode (λ_s) and this mode is taken to its high-temperature limit. See also Eq. (A5) of this Comment.
21. (a) The individual thermally weighted Franck–Condon factors, $fc(m_c, m_f)$, for the three-mode case are defined by Eqs. (2), (13a) and by

$$\overline{\mathrm{FC}} = \sum_{mf=0}^{\infty} \sum_{mc=-\infty}^{\infty} \mathrm{fc}(\mathrm{m_c},\mathrm{m_f})$$

(b) An alternative approach, similar to that used to derive Eqs. (10c) and (10d), can be used to derive a closed-form expression for the rate constant for the three-mode case. In this approach the double sum in Eq. (13b) is approximated by the product of the maximum value of the function, the widths of the Gaussians for the intermediate and high-frequency modes, and a normalizing factor. A typical distribution of the terms that contribute to the sum and the width of the distribution is shown in Figs. 9(a) and 9(b). (c) For adiabatic reactions the rate constant is equal to the product of a (nuclear) frequency and a nuclear factor. In this case the introduction of a high-frequency mode can substantially increase the frequency factor, and therefore the rate constant, even in the normal region (see Ref. 10).
22. A. Sarai, Chem. Phys. Lett. **63**, 360 (1979): A. Sarai and T. Kakitani, Chem. Phys. Lett. **77**, 427 (1981).
23. E. Buhks, G. Navon, M. Bixon and J. Jortner, J. Am. Chem. Soc. **102**, 2918 (1980).
24. M. Bixon and J. Jortner, J. Phys. Chem. **90**, 3795 (1986). S. E. Peterson-Kennedy, J. L. McGourty, J. A. Kalweit and B. M. Hoffman, J. Am. Chem. Soc. **108**, 1739 (1986). A. Sarai, Biochim. Biophys. Acta **71**, 589 (1980).
25. K. F. Freed and J. Jortner, J. Chem. Phys. **52**, 6272 (1970).